Title	ON DIAGRAMS OF SIMPLIFIED TRISECTIONS AND MAPPING CLASS GROUPS
Author(s)	Hayano, Kenta
Citation	Osaka Journal of Mathematics. 2020, 57(1), p. 17-37
Version Type	VoR
URL	https://doi.org/10.18910/73735
rights	
Note	

ON DIAGRAMS OF SIMPLIFIED TRISECTIONS AND MAPPING CLASS GROUPS

Kenta HAYANO

(Received November 22, 2017, revised June 13, 2018)

Abstract

A simplified trisection is a trisection map on a 4–manifold such that, in its critical value set, there is no double point and cusps only appear in triples on innermost fold circles. We give a necessary and sufficient condition for a 3–tuple of systems of simple closed curves in a surface to be a diagram of a simplified trisection in terms of mapping class groups. As an application of this criterion, we show that trisections of spun 4–manifolds due to Meier are diffeomorphic (as trisections) to simplified ones. Baykur and Saeki recently gave an algorithmic construction of a simplified trisection from a directed broken Lefschetz fibration. We also give an algorithm to obtain a diagram of a simplified trisection derived from their construction.

1. Introduction

A *trisection*, due to Gay and Kirby [9], is a decomposition of a 4–manifold into three 4-dimensional handlebodies, which can be considered as a 4–dimensional counterpart of a Heegaard splitting of a 3–manifold. Indeed, we can obtain a 4–manifold with a trisection from a 3–tuple of systems of simple closed curves in a closed surface, which is called a *trisection diagram*, as we can obtain a 3–manifold with a Heegaard splitting from a Heegaard diagram. On the other hand, we can also obtain a trisection of a 4–manifold from a stable map to the plane with a specific configuration of the critical value set (see Figure 2), which we will call a *trisection map* (or a trisection for simplicity).

In studying smooth maps from 4–manifolds to surfaces with stable and Lefschetz singularities, Baykur and Saeki [6] introduced *simplified trisections*, which are trisection maps such that in their critical value sets, there are no double points and cusps only appear in triples on innermost fold circles (see Figure 3 for the critical value set of a simplified trisection). They further gave an algorithm to obtain simplified trisections from directed broken Lefschetz fibrations, which implies the existence of a simplified trisection for an arbitrary 4–manifold. In this paper, relying on the theory of mapping class groups of surfaces, we study trisection diagrams associated with simplified trisections.

We first discuss when a 3–tuple of (ordered) systems of simple closed curves is a diagram associated with a simplified trisection in terms of mapping class groups. Since the critical value set of a simplified trisection is nested circles with cusps (see Figure 3), we can take a monodromy along a loop between each consecutive pair of components in the critical value set. We will simultaneously give an algorithm to determine such a monodromy from curves in a diagram of a simplified trisection, and a necessary and sufficient condition for

2010 Mathematics Subject Classification. Primary 57R45; Secondary 20F38, 57M99, 57R65.

a given 3–tuple of systems of curves to be a diagram associated with a simplified trisection (Theorem 3.4 and Lemma 3.5). Note that, strictly speaking, these results do not directly explain relation between simplified trisections and their diagrams: the curves a_i, b_j, c_j in Theorem 3.4 are not curves in a trisection diagram, but vanishing cycles of indefinite folds of a simplified trisection (see the second paragraph of Section 3). We will clarify relation between the vanishing cycles in Theorem 3.4 and curves in a diagram of a simplified trisection (Proposition 3.1). As an application of the results, we will show that trisections of spun 4–manifolds constructed by Meier [13] are diffeomorphic to simplified trisections (Theorem 3.7). We will also classify simplified trisections with genus 2 using Theorem 3.4 (Theorem 3.9). This classification can also be obtained as merely a corollary of the classification of genus–2 trisections given in [14], in which the authors relied on deep results on genus–2 Heegaard splittings of S^3, while we will reduce the classification to linear algebraic problems, which is easy to solve.

By analyzing how vanishing cycles are changed in algorithmic construction of simplified trisections from broken Lefschetz fibrations given in [6], we next give an algorithm to obtain trisection diagrams from vanishing cycles of broken Lefschetz fibrations. In the analysis of vanishing cycles, we will be faced with problems concerning how parallel transports are affected by homotopies of stable maps called R2–moves, which change the critical value sets like the Reidemeister move of type II. We will solve such problems by making use of the results by the author [12], which completely describe the effect of R2–moves on parallel transports (and thus that on vanishing cycles) in terms of mapping class groups. Lastly we will apply the algorithm to genus–1 simplified broken Lefschetz fibrations, resulting in diagrams associated with simplified trisections on S^4, the connected sum of $S^1 \times S^3$ and an S^2–bundle over S^2, and manifolds L_n and L'_n due to Pao [15] (Example 4.6). Using the diagram obtained there, we will verify that a simplified $(3, 1)$–trisection on S^4 obtained from a genus–1 simplified broken Lefschetz fibration is diffeomorphic to the stabilization of the $(0, 0)$–trisection of S^4 (Figure 20 explicitly gives sequences of handle-slides between diagrams corresponding to the two trisections).

2. Preliminaries

Throughout the paper, we will assume that any manifold is smooth, connected, compact and oriented unless otherwise noted. We will describe the image of definite (resp. indefinite) folds by red (resp. black) curves with co-orientations as shown in Figures 1(1) and 1(2). As shown in Figure 1(3), we will describe the image of a Lefschetz singularity by a cross. Note that these conventions are the same as those in [6].

2.1. Mapping class groups and monodromies along indefinite folds. Let Σ be a surface, $V_1, \ldots, V_k \subset \Sigma$ discrete subsets, and $c_1, \ldots, c_l$ simple closed curves. We denote the set of orientation preserving diffeomorphisms fixing $V_1, \ldots, V_k$ setwise by $\mathrm{Diff}^+(\Sigma; V_1, \ldots, V_k)$, and we put

$$\mathrm{Mod}(\Sigma; V_1, \ldots, V_k)(c_1, \ldots, c_l) = \left\{ [\varphi] \in \pi_0\left(\mathrm{Diff}^+(\Sigma; V_1, \ldots, V_k)\right) \middle| \varphi(c_i) = c_i \ (i = 1, \ldots, l) \right\}.$$

We endow it with a group structure by compositions of representatives. Let Σ_{c_i} be a surface obtained by applying surgery along c_i (i.e. attaching two disks to $\Sigma \setminus \nu(c_i)$, where $\nu(c_i) \subset \Sigma$ is a tubular neighborhood of c_i), and $v_0, v'_0 \in \Sigma_{c_i}$ the centers of the disks. We define a *(pointed)*
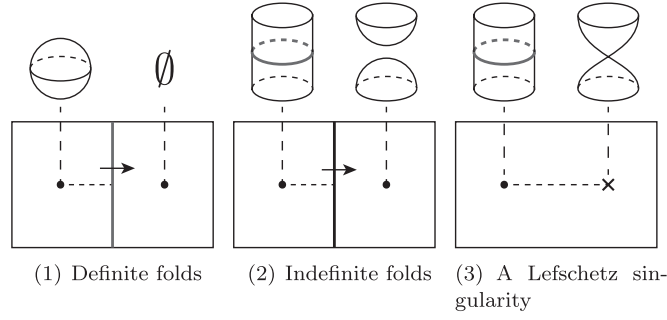
(1) Definite folds   (2) Indefinite folds   (3) A Lefschetz singularity

Fig. 1. Fibers around critical values.

surgery homomorphism

$$\Phi^*_{c_i} : \mathrm{Mod}(\Sigma; V_1, \ldots, V_k)(c_1, \ldots, c_l) \to \mathrm{Mod}(\Sigma_{c_i}; \{v_0, v'_0\}, V_1, \ldots, V_k)(c_1, \ldots, c_{i-1}, c_{i+1}, \ldots, c_l)$$

as follows. For an element $\varphi \in \mathrm{Diff}^+(\Sigma; V_1, \ldots, V_k)$, we first modify φ by an isotopy so that it preserves $\nu(c_i)$. Let $\tilde{\varphi} : \Sigma_{c_i} \to \Sigma_{c_i}$ be an extension of the diffeomorphism $\varphi|_{\Sigma \setminus \nu(c_i)}$ preserving the set $\{v_0, v'_0\}$. We then put $\Phi^*_{c_i}([\varphi]) = [\tilde{\varphi}]$. It is known that the map $\Phi^*_{c_i}$ is well-defined and the kernel of $\Phi^*_{c_i}$ is generated by the Dehn twist t_{c_i} (for the proof, see [4, Lemma 3.1]*, for example). We put $\Phi_{c_i} = F_{v_0, v'_0} \circ \Phi^*_{c_i}$, which is also called a *surgery homomorphism*, where F_{v_0, v'_0} is the forgetting map.

Let $f : X \to \Sigma$ be a smooth map on a 4–manifold to a surface and $S \subset \mathrm{Crit}(f)$ be a circle consisting of indefinite folds. Assume that the restriction $f|_S$ is embedding and the complement $\nu(f(S)) \setminus f(S)$, where $\nu(f(S))$ is a tubular neighborhood of $f(S)$, does not contain any critical values of f. The complement $\nu(f(S)) \setminus f(S)$ has two components. We take two points p_0, q_0 from each of the components. Let α and β be loops in $\nu(f(S)) \setminus f(S)$ based at p_0 and q_0, respectively, such that these curves represent the same element in $H_1(\nu(f(S)); \mathbb{Z})$. We take an oriented simple path $\gamma \subset \nu(f(S))$ from p_0 to q_0 intersecting with $f(S)$ on one point transversely. Assume that the orientation of γ coincides with the co-orientation of $f(S)$ at the intersection. The arc γ gives rise to a vanishing cycle $c \subset \Sigma = f^{-1}(p_0)$ and an identification of $f^{-1}(q_0)$ with Σ_c. It is known that the monodromy $\mu \in \mathrm{Mod}(\Sigma)$ along α is contained in $\mathrm{Mod}(\Sigma)(c)$ and, under the identification above, the monodromy along β is equal to $\Phi_c(\mu)$ (see [3, 4]).

2.2. Trisections of 4–manifolds. Let X be a closed 4–manifold. A decomposition $X = X_1 \cup X_2 \cup X_3$ is called a (g, k)–*trisection* if

- for each $i = 1, 2, 3$, there is a diffeomorphism $\phi_i : X_i \to \natural^k(S^1 \times D^3)$, and
- for each $i = 1, 2, 3$, taking indices mod 3, $\phi_i(X_i \cap X_{i+1}) = Y^-_{k,g}$ and $\phi_i(X_i \cap X_{i-1}) = Y^+_{k,g}$, where $\partial \left(\natural^k(S^1 \times D^3) \right) = \#^k(S^1 \times S^2) = Y^+_{k,g} \cup Y^-_{k,g}$ is a Heegaard splitting of $\#^k(S^1 \times S^2)$ obtained by stabilizing the standard genus–k Heegaard splitting $g - k$ times.

A stable map $f : X \to \mathbb{R}^2$ is called a (g, k)–*trisection map* if its critical value set is as shown in Figure 2, where each of the three white boxes, called a *Cerf box* of f, consists of a Cerf graphic without cusps and definite folds (i.e. it consists of indefinite fold images with transverse double points but without "radial tangencies"). A trisection map f is said

---

*The authors merely dealt with the case $k = 0$ and $l = 1$ in [4], yet the proof there works for general cases.

to be *simplified* if its Cerf boxes do not contain double points. Note that, by the definition of a simplified trisection, cusps of it only appear in triples on innermost fold circles (see Figure 3). Let α, β, γ be g–tuples of simple closed curves in Σ_g. A tuple $(\Sigma_g; \alpha, \beta, \gamma)$ is called
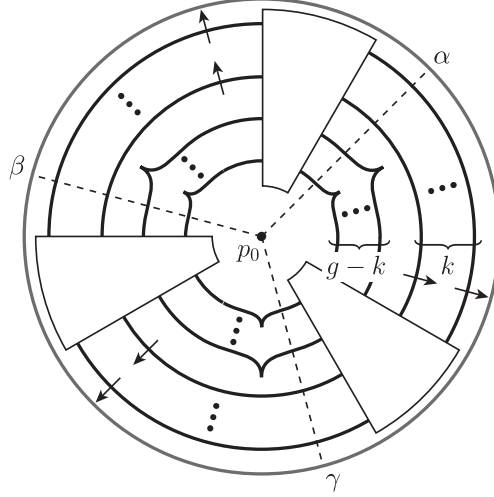

Fig. 2. The critical value set of a trisection map.

a (g, k)–*trisection diagram* if each of the tuples $(\Sigma_g; \alpha, \beta), (\Sigma_g; \beta, \gamma)$ and $(\Sigma_g; \gamma, \alpha)$ is a genus–g Heegaard diagram of $\natural^k(S^1 \times S^2)$. In this paper we will mainly focus on trisection maps and diagrams. For this reason, we will sometimes call trisection maps just trisections for simplicity.

From a (g, k)–trisection map $f : X \to \mathbb{R}^2$, we can obtain a trisection of X and a trisection diagram as follows. The three dotted segments in Figure 2 decomposes the image of f into three regions D_1, D_2 and D_3. The decomposition $X = X_1 \cup X_2 \cup X_3$ is a (g, k)–trisection of X, where $X_i = f^{-1}(D_i)$. Furthermore, by taking vanishing cycles of f with respect to the three dotted segments in Figure 2, we can obtain a three g–tuples $\alpha = (\alpha_1, \ldots, \alpha_g), \beta = (\beta_1, \ldots, \beta_g), \gamma = (\gamma_1, \ldots, \gamma_g)$ of simple closed curves in $f^{-1}(p_0) \cong \Sigma_g$. The tuple $(\Sigma_g; \alpha, \beta, \gamma)$ is a (g, k)–trisection diagram.

Conversely, for a (g, k)–trisection diagram $(\Sigma_g; \alpha, \beta, \gamma)$ (or a (g, k)–trisection of X), there exists a (g, k)–trisection map $f : X \to \mathbb{R}^2$ such that the corresponding diagram obtained in the procedure above is $(\Sigma_g; \alpha, \beta, \gamma)$. Note that the diffeomorphism type of X is uniquely determined from the diagram $(\Sigma_g; \alpha, \beta, \gamma)$, while a trisection map f is not uniquely determined (there are many choices of Cerf boxes, for example).

Two trisections $X = X_1 \cup X_2 \cup X_3$ and $X' = X'_1 \cup X'_2 \cup X'_3$ are said to be *diffeomorphic* if there exists an orientation preserving diffeomorphism $\Phi : X \to X'$ sending X_i to X'_i. It is known that two trisections of the same manifold become diffeomorphic after stabilizing each trisection several times (for the definition of stabilization and the proof of this statement, see [9]). Since any two handle decompositions of a genus–g handlebody with one 0–handle and g 1–handles are related by handle-slides, two trisections are diffeomorphic if and only if the corresponding diagrams are related by orientation preserving self-diffeomorphisms of Σ_g and handle-slides, which are slides of α– (resp. β– and γ–) curves over α– (resp. β– and γ–) curves.

3. Description of simplified trisections via mapping class groups

As we briefly reviewed in Section 2.2, three g–tuples α, β, γ of simple closed curves in Σ_g is a (g, k)–trisection diagram if and only if each two of the tuples is a genus–g Heegaard diagram of $\sharp^k(S^1 \times S^2)$. In this section, after observing relation between diagrams and vanishing cycles of simplified trisections (Proposition 3.1), we will give a necessary and sufficient condition for systems of simple closed curves to be vanishing cycles of a *simplified* (g, k)–trisection in terms of mapping class groups. Making use of this condition, we will then show that trisections of spun 4–manifolds constructed by Meier [13] are diffeomorphic to simplified ones (Theorem 3.7). We will also give an elementary proof (without relying on the more general result in [14]) of the classification of simplified trisections with genus 2 (Theorem 3.9).

Let $f : X \to \mathbb{R}^2$ be a simplified (g, k)–trisection. We take reference paths in $\mathbb{R}^2$ as shown by dotted segments in Figure 3. We denote the fiber on the center by Σ. Let $a_i, b_i, c_i \subset \Sigma$ be vanishing cycles of the i–th innermost indefinite fold circle associated with the reference paths in Figure 3. In what follows, the vanishing cycles are assumed to be in general position. Note that a_i, b_i and c_i are unique up to isotopies and handle-slides over $a_1, \ldots, a_{i-1}$. Following the observation in [6, Remark 7.2], we call such handle-slides *upper-triangular handle-slides*.
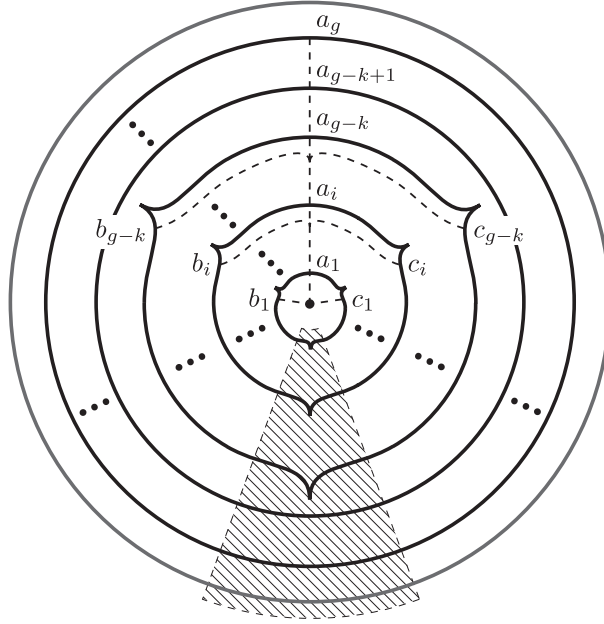

Fig. 3. Reference paths for a simplified (g, k)–trisection.

Proposition 3.1. *We can obtain a trisection diagram $(\Sigma; \alpha, \beta, \gamma)$ associated with f by taking $\alpha_i, \beta_i, \gamma_i$ as follows:*

- *for each $i = 1, \ldots, g$, $\alpha_i = a_i$,*
- *for each $j = 1, \ldots, g - k$, β_j (resp. γ_j) is a curve obtained by applying upper-triangular handle-slides to b_j (resp. c_j) so that the resulting curve is disjoint from the curves $b_1, \ldots, b_{j-1}$ (resp. $c_1, \ldots, c_{j-1}$),*

- *for each $l = g - k + 1, \ldots, g$, β_l (resp. γ_l) is a curve obtained by applying upper-triangular handle-slides to a_l so that the resulting curve is disjoint from $b_1, \ldots, b_{l-1}$ (resp. $c_1, \ldots, c_{l-1}$),*

Conversely, let $(\Sigma; \alpha', \beta', \gamma')$ be a trisection diagram associated with a simplified (g, k)–trisection f' and a'_i, b'_j, c'_j ($i = 1, \ldots, g$, $j = 1, \ldots, g - k$) vanishing cycles associated with the reference paths in Figure 3. *Then the followings hold up to upper-triangular handle-slides:*

- *for each $i = 1, \ldots, g$, $a'_i = \alpha'_i$,*
- *for each $j = 1, \ldots, g - k$, b'_j (resp. c'_j) is equal to a curve obtained by applying upper-triangular handle-slides to β'_j (resp. γ'_j) so that the resulting curve is disjoint from the curves $\beta'_1, \ldots, \beta'_{j-1}$ (resp. $\gamma'_1, \ldots, \gamma'_{j-1}$),*
- *for each $l = g - k + 1, \ldots, g$, $\alpha'_l = \beta'_l = \gamma'_l$.*

Proposition 3.1 can be deduced immediately from the following lemma:

Lemma 3.2. *Let d_1, d_2, d_3, d_4 be vanishing cycles associated with the corresponding reference paths around two consecutive cusps as shown in* Figure 4(1). *The curve d_4 is isotopic to $t^{-1}_{t_{d_1}(d_2)}(d_3)$. In particular d_3 and d_4 are isotopic if d_3 is disjoint from d_2.*
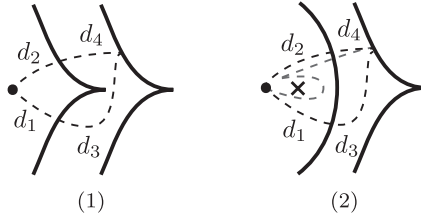

Fig. 4. Reference paths around two consecutive cusps.

REMARK 3.3. Since d_1 and d_2 intersect on one point, we can always make d_3 disjoint from d_2 by applying handle-slides over d_1.

Proof of Lemma 3.2.   Applying unsink to the left cusp in Figure 4(1), we obtain a new map whose critical value set is shown in Figure 4(2). The curve d_3 is isotopic to a vanishing cycle associated with the red reference path in Figure 4(2). Thus, d_3 is sent to d_4 by the Dehn twist along the curve $t_{d_1}(d_2)$.   □

We are now ready for giving a criterion for a system of simple closed curves to be a diagram of a simplified trisection, in terms of the corresponding vanishing cycles.

Theorem 3.4. *Vanishing cycles $a_1, \ldots, a_g, b_1, \ldots, b_{g-k}, c_1, \ldots, c_{g-k}$ of a simplified (g, k)–trisection taken as above satisfy the following conditions:*

(1) *the curves b_i and c_i intersect with a_i on one point for each $i = 2, \ldots, g - k$,*

(2) *for any $i \in \{0, \ldots, g - k - 1\}$, $c'_{i+1} = \mu_i^{-1}(c_{i+1})$ intersects b_{i+1} on one point, where $\Sigma_{a_1, \ldots, a_i} = (\Sigma_{a_1, \ldots, a_{i-1}})_{a_i}$ and $\mu_i \in \mathrm{Mod}(\Sigma_{a_1, \ldots, a_i})$ is inductively defined as*

$$\mu_i = \begin{cases} [\mathrm{id}_\Sigma] & (i = 0) \\ \Phi_{a_i}(t_{t_{c_i a_i}} \circ \mu_{i-1} \circ t_{t_{b_i c'_i}} \circ t_{t_{a_i b_i}}) & (i > 0). \end{cases}$$

(Note that $t_{t_{c_i}a_i} \circ \mu_{i-1} \circ t_{t_{b_i}c'_i} \circ t_{t_{a_i}b_i}$ preserves a_i if c'_i intersects b_i on one point. In particular the condition for i makes sense if that for $i-1$ holds.)

(3) *for any $j \in \{g - k, \ldots, g - 1\}$, $\Phi_{a_j} \circ \cdots \circ \Phi_{a_{g-k+1}}(\mu_{g-k})$ preserves a_{j+1}.*

Conversely, for three sequences of curves $\{a_1, \ldots, a_g\}, \{b_1, \ldots, b_{g-k}\}, \{c_1, \ldots, c_{g-k}\}$ satisfying the conditions above (such that b_i and c_i are disjoint from $a_1, \ldots, a_{i-1}$), there exists a simplified (g, k)–trisection $f' : X' \to \mathbb{R}^2$ whose vanishing cycles associated with the reference paths in Figure 3 *are $a_1, \ldots, a_g, b_1, \ldots, b_{g-k}, c_1, \ldots, c_{g-k}$.*

We will obtain vanishing cycles of several simplified trisections in the next section. For example, the red and blue curves in Figure 18(2) (which are a_1, a_2, a_3 and b_1, b_2, respectively) and the green curves labeled with 1 and 2 in Figure 19(3) (which are c_1, c_2) are vanishing cycles of a simplified trisection on S^4. We can easily check that these curves satisfy the conditions in Theorem 3.4.

We need the following lemma to prove Theorem 3.4.

Lemma 3.5. *The mapping class μ_i defined in* Theorem 3.4 *is the monodromy along a loop (with counterclockwise orientation) obtained by pushing the i–th innermost circle to the inside of it.*

Proof. We prove the lemma by induction on i. The statement is obvious for $i = 0$. Assume that the lemma holds for $i = j - 1$, where $j \leq g - k - 1$. The curve $c'_i = \mu_{i-1}^{-1}(c_i)$ is a vanishing cycle of f associated with the reference path shown in Figure 5(1). We apply unsinks to the
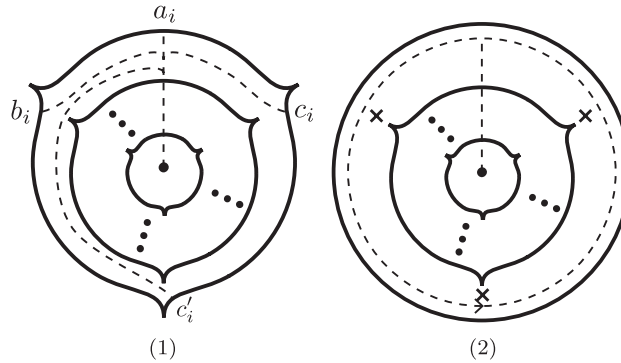

Fig. 5. Reference paths for (1) vanishing cycles a_i, b_i, c_i, c'_i and (2) a monodromy $t_{t_{c_i}a_i} \circ \mu_{i-1} \circ t_{t_{b_i}c'_i} \circ t_{t_{a_i}b_i}$.

three cusps on the i–th innermost fold circles. The critical value set of the resulting map is shown in Figure 5(2). Vanishing cycles of the three Lefschetz singularities are respectively equal to $t_{a_i}(b_i), t_{b_i}(c'_i)$ and $t_{c_i}(a_i)$. Thus the monodromy along the dotted curve in Figure 5(2) is equal to $t_{t_{c_i}a_i} \circ \mu_{i-1} \circ t_{t_{b_i}c'_i} \circ t_{t_{a_i}b_i}$. The statement then follows from the observation in Section 2.1. Lastly, the statement for μ_j with $j \geq g - k$ also follows from the observation in Section 2.1, together with the induction hypothesis. □

Proof of Theorem 3.4. Let $a_1, \ldots, a_g, b_1, \ldots, b_{g-k}, c_1, \ldots, c_{g-k}$ be vanishing cycles of a simplified (g, k)–trisection taken as above. The condition (1) holds since two vanishing cycles of indefinite folds around a cusp intersect on one point, while the conditions (2) and (3) immediately follow from Lemma 3.5.

In order to prove the latter part of Theorem 3.4, suppose that three systems of curves $(a_1,\ldots,a_g),(b_1,\ldots,b_{g-k}),(c_1,\ldots,c_{g-k})$ satisfy the conditions in the theorem. The condition (1) guarantees existence of a map $f_1 : X_1 \to \mathbb{R}^2$, where X_1 is a 4–manifold with boundary, such that the critical value set of f_1 is the same as that in the complement of the shaded region in Figure 3 and it has the desired vanishing cycles $a_1,\ldots,a_g,b_1,\ldots,b_{g-k},c_1\ldots,c_{g-k}$. We can inductively see that the condition (2) (together with Lemma 3.5) guarantees that we can attach $g - k$ cusps in the shaded region to f_1, and the condition (3) (together with Lemma 3.5) further guarantees that the resulting map can be extended to the all of the shaded region. $\qquad\square$

For applications of Theorem 3.4, we need to describe the monodromy μ_{i+1} of a simplified trisection as a product of Dehn twists under the assumption that the inner monodromy μ_i is trivial:

Lemma 3.6. *Let $f : X \to \mathbb{R}^2$ be a simplified trisection. Suppose that the monodromy μ_i obtained as in* Theorem 3.4 *is trivial. We denote $\Sigma_{a_1,\ldots,a_i}$ by Σ and a_{i+1} (resp. b_{i+1}, c_{i+1}) by a (resp. b, c) for simplicity.*

(1) *A regular neighborhood of $a \cup b \cup c$ is a genus–1 surface with three boundary components.*

(2) *The monodromy μ_{i+1} is $t_{\delta_1}^2 t_{\delta_3}^2 t_{\delta_2}^{-1}$ if we can take orientations of a, b and c so that the algebraic intersections $a \cdot b$, $b \cdot c$ and $c \cdot a$ are all equal to 1 (Figure 6(1)), and is equal to $t_{\delta_1}^{-2} t_{\delta_3}^{-2} t_{\delta_2}$ otherwise (Figure 6(2)).*
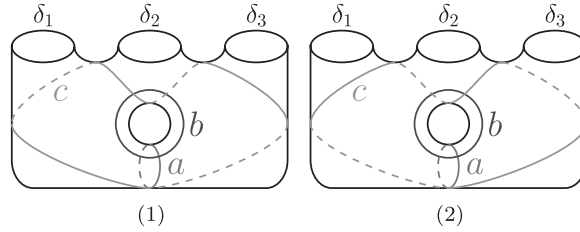

Fig. 6. Two possibilities of configurations of vanishing cycles of f.

Proof. The first statement immediately follows from Theorem 3.4 and the assumption (note that each two of the curves a, b, c intersect on one point). Since the monodromy μ_{i+1} becomes the inverse of it when we change the orientation of X (and thus that of Σ), it is enough to show the statement under the assumption that we can take orientations of a, b and c so that the algebraic intersections $a \cdot b$, $b \cdot c$ and $c \cdot a$ are all equal to 1 (i.e. a, b and c are as shown in Figure 6(1)). In what follows, for (an isotopy class of) a simple closed curve d in Σ, we also denote the Dehn twist along it by d (which is contained in $\mathrm{Mod}(\Sigma; \partial\Sigma)$). For an element $\varphi \in \mathrm{Mod}(\Sigma; \partial\Sigma)$, let $_\varphi(d)$ be the isotopy class of a simple closed curve in Σ represented by the image of d by a representative of φ.

We take simple closed curves x and y as shown in Figure 7. By Lemma 3.5 and the assumption, the monodromy μ_{i+1} is equal to $\Phi_a(_c(a)_b(c)_a(b))$. Since the curve c is equal to $_{xy\bar{a}}(b)$, we can calculate $_c(a)_b(c)_a(b)$ as follows (in the following calculation, the only underlined part in each line is changed when proceeding to the next line):
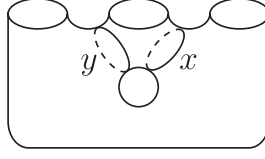
Fig. 7. Simple closed curves in a neighborhood of $a \cup b \cup c$.

$$
\begin{aligned}
{}_c(a)_b(c)_a(b) &= \underline{c}a\underline{c} \cdot b\underline{c}\overline{b} \cdot ab\overline{a} \\
&= (xy\overline{a}b\overline{xy}a) \cdot a \cdot (xy\overline{a}\overline{b}\overline{xy}a) \cdot b \cdot (xy\overline{a}b\overline{xy}a) \cdot \overline{b} \cdot ab\overline{a} \\
&= xy\underline{a}b \cdot (a) \cdot \overline{b}\overline{xy}abxy\overline{a} \cdot ({}_b(\overline{x})_b(\overline{y})b)(a^2b\overline{a}^2) \\
&= xy \cdot (\overline{a}^2ba) \cdot \overline{xy}ab \cdot (\overline{a}x\overline{b}y \cdot {}_b(\overline{x})) \cdot (\Delta_{a,b}\overline{a}^4) \\
&= xy\overline{a}^2ba\overline{xy} \cdot (\overline{b}a\overline{x}bx) \cdot y_b(\overline{x})\Delta_{a,b}\overline{a}^4 \\
&= xy\overline{a}^2ba\overline{xy}ba\overline{x}b \cdot (y\overline{b}x) \cdot \Delta_{a,b}\overline{a}^4 \\
&= xy\overline{a}^2ba\overline{x} \cdot (\overline{b}\overline{y}\underline{bab}\,\overline{b}\overline{x}by) \cdot x\Delta_{a,b}\overline{a}^4 \\
&= xy\overline{a}^2ba\overline{x}\overline{b}\overline{y} \cdot (aba\overline{a}^2x\overline{b}x) \cdot yx\Delta_{a,b}\overline{a}^4 \\
&= xy\overline{a}^2ba\overline{x} \cdot (y\overline{b}\overline{y}\underline{a}b) \cdot \overline{a}^2x\overline{b}\overline{x}yx\Delta_{a,b}\overline{a}^4 \\
&= xy\overline{a}^2\underline{ba\overline{x}y\overline{b}\overline{y}} \cdot (x\overline{a}\overline{b}ba^2\overline{x}) \cdot b\overline{a}^2x\overline{b}\overline{x}yx\Delta_{a,b}\overline{a}^4 \\
&= xy\overline{a}^2 \cdot {}_{ba\overline{x}y}(\overline{b}) \cdot {}_{ba^2\overline{x}}(b) \cdot \overline{x}yx\Delta_{a,b}\overline{a}^4,
\end{aligned}
$$

where we denote the product $(ab)^3$ by $\Delta_{a,b}$. We can easily check that the curves ${}_{ba\overline{x}y}(b)$ and ${}_{ba^2\overline{x}}(b)$ are as shown in Figure 8. These curves are disjoint from the curve a, in particular

(1) The curve ${}_{ba\overline{x}y}(b)$.   (2) The curve ${}_{ba^2\overline{x}}(b)$.
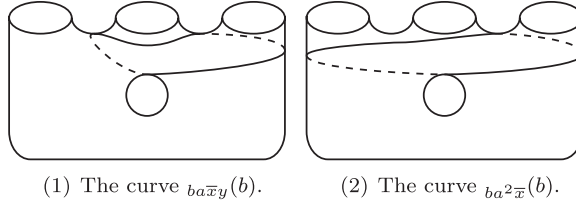
Fig. 8. Simple closed curves in a neighborhood of $a \cup b \cup c$.

the Dehn twists along them are contained in $\mathrm{Mod}(\Sigma)(a)$. The map Φ_a sends the Dehn twists along ${}_{ba\overline{x}y}(b)$ and ${}_{ba^2\overline{x}}(b)$ to t_{δ_2} and t_{δ_3}, respectively. We can thus calculate the monodromy $\Phi_a({}_c(a)_b(c)_a(b))$ as follows:

$$
\begin{aligned}
\Phi_a({}_c(a)_b(c)_a(b)) &= \Phi_a(xy\overline{a}^2 \cdot {}_{ba\overline{x}y}(\overline{b}) \cdot {}_{ba^2\overline{x}}(b) \cdot \overline{x}yx\Delta_{a,b}\overline{a}^4) \\
&= \delta_3\delta_1\overline{\delta_2}\delta_3\overline{\delta_3}\delta_1\delta_3 = \delta_1^2\overline{\delta_2}\delta_3^2.
\end{aligned}
$$

This completes the proof. $\qquad\square$

Meier [13] constructed a $(3g, g)$–trisection of the spun manifold $S(M)$ of a 3–manifold M with a genus–g Heegaard splitting. He also gave an algorithm to obtain a trisection diagram of it from a Heegaard diagram of M. Using Theorem 3.4, together with this algorithm, we

can prove:

Theorem 3.7. *Meier's trisection on $\mathcal{S}(M)$ is diffeomorphic to one associated with a simplified trisection.*

Proof. Let $(\Sigma_g; \delta, \varepsilon)$ be a genus–g Heegaard diagram of M such that ε–curves are in the standard position (see Figure 9). According to [13, Theorem 1.4], a trisection diagram of
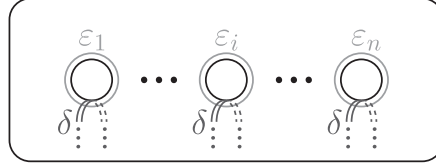

Fig. 9. A standard Heegaard diagram.

the spun manifold $\mathcal{S}(M)$ can be obtained by replacing a neighborhood of each ε_i in the Heegaard diagram $(\Sigma_g; \delta, \varepsilon)$ (which is shown in Figure 10(1)) with a genus–3 surface and curves given in Figures 10(2), 10(3) and 10(4), where $\alpha_\delta = \{\alpha_{\delta_1}, \ldots, \alpha_{\delta_g}\}$ and α_{δ_j} coincides with δ_j outside of the union of neighborhoods of ε_i's. We will show that the curves $\alpha_1, \ldots, \alpha_{2g}, \alpha_{\delta_1}, \ldots, \alpha_{\delta_g}, \beta_1, \ldots, \beta_{2g}, \gamma_1, \ldots, \gamma_{2g}$ satisfy the conditions in Theorem 3.4. The statement then follows immediately from Proposition 3.1. The first condition is obvious,
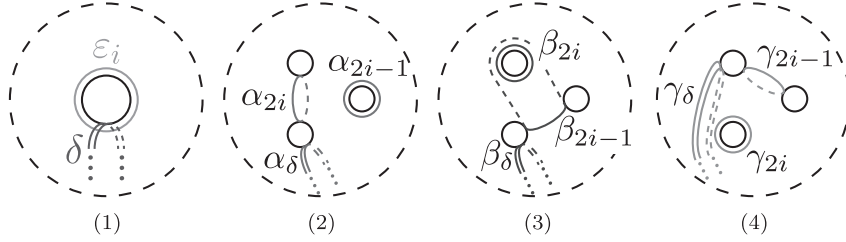

Fig. 10. Curves in a trisection diagram of $\mathcal{S}(M)$.

while we can easily deduce the second and the third conditions from the following claim:

Claim. *The element $\mu_i \in \mathrm{Mod}(\Sigma_{\alpha_1,\ldots,\alpha_i})$ determined from $\alpha_1, \ldots, \alpha_{2g}, \beta_1, \ldots, \beta_{2g}, \gamma_1, \ldots, \gamma_{2g}$ is equal to the Dehn twist along $t_{\beta_{i+1}}(\alpha_{i+1})$ if i is odd, and equal to the identity if i is even.*

The claim is obvious for $i = 0$. Suppose that the claim holds for $i = 2k - 2$. Each two of the curves $\alpha_{2k-1}, \beta_{2k-1}, \gamma_{2k-1}$ intersect on one point. One of the boundary component of a regular neighborhood of $\alpha_{2k-1} \cup \beta_{2k-1} \cup \gamma_{2k-1}$ bounds a disk, while the other components are isotopic to $t_{\beta_{2k}}(\alpha_{2k})$. Thus, we can deduce from Lemma 3.6 that μ_{2k-1} is equal to the Dehn twist along $t_{\beta_{2k}}(\alpha_{2k})$ (note that we can take orientations of $\alpha_{2k-1}, \beta_{2k-1}, \gamma_{2k-1}$ so that the algebraic intersections $\alpha_{2k-1} \cdot \beta_{2k-1}, \beta_{2k-1} \cdot \gamma_{2k-1}$ and $\gamma_{2k-1} \cdot \alpha_{2k-1}$ are all equal to 1).

For simplicity, we denote $\alpha_{2k}, \beta_{2k}, \gamma_{2k}$ by α, β, γ, respectively. It is easy to see that the curve $\gamma' = \mu_{2k-1}^{-1}(\gamma)$ intersects with β on one point. Thus, we can calculate the monodromy μ_{2k} as follows (in the following calculation, the only underlined part in each line is changed when proceeding to the next line):

$$
\begin{aligned}
\mu_{2k} &= \Phi_\alpha\left({}_\gamma(\alpha) \cdot \mu_{2k-1} \cdot {}_\beta(\gamma') \cdot {}_\alpha(\beta) \right) \\
&= \Phi_\alpha\left(\gamma\alpha\overline{\gamma} \cdot \beta\alpha\overline{\beta} \cdot \beta\gamma'\overline{\beta} \cdot \alpha\beta\overline{\alpha} \right) \\
&= \Phi_\alpha\left((\overline{\alpha}\gamma\alpha) \cdot \beta\alpha \cdot (\overline{\mu_{2k-1}}\gamma\mu_{2k-1}) \cdot (\alpha\beta\overline{\alpha}^2) \right) \\
&= \Phi_\alpha\left(\gamma\alpha\beta\alpha \cdot (\beta\overline{\alpha}\overline{\beta}) \cdot \gamma \cdot (\beta\alpha\overline{\beta}) \cdot \alpha\beta \right) \qquad \text{(Note that } \alpha \in \text{Ker}(\Phi_\alpha).\text{)} \\
&= \Phi_\alpha\left(\gamma\alpha \cdot \alpha \cdot \gamma\beta\alpha \cdot (\alpha\beta\overline{\alpha}) \right) \\
&= \Phi_\alpha\left(\overline{\alpha}^2(\alpha\gamma)^3(\alpha\beta)^3\overline{\alpha}^3 \right) = 1.
\end{aligned}
$$

This completes the proof of the claim. □

REMARK 3.8. In Section 4 we will also obtain a diagram of a simplified $(3, 1)$–trisection of $L_p \cong S(L(p,q))$ constructed from a genus–1 simplified broken Lefschetz fibration on it (see Example 4.6). Although some of such simplified trisections (e.g. those of S^4 and $S^1 \times S^3 \sharp S^2 \times S^2$) are diffeomorphic to those constructed by Meier [13], the author does not know whether *any* simplified trisection obtained from a genus–1 simplified broken Lefschetz fibration is diffeomorphic to that obtained from a genus–1 Heegaard splitting of some lens space.

Another application of Theorem 3.4 is the classification of 4–manifolds admitting genus–2 simplified trisections:

Theorem 3.9. *A 4–manifold X admits a genus–2 simplified trisection if and only if X is diffeomorphic to either $S^2 \times S^2$ or a connected sum of $\mathbb{CP}^2$, $\overline{\mathbb{CP}}^2$ and $S^1 \times S^3$ with two summands.*

As we noted in the beginning of the section, we can deduce this theorem as merely a corollary of the classification of genus–2 general trisections in [14]. Although we only deal with simplified trisections, our proof below relies on easy linear-algebraic calculations, while that in [14] involves subtle arguments on configurations of curves in genus–2 surfaces.

Proof of Theorem 3.9. Since $S^1 \times S^3$, $\mathbb{CP}^2$ and $\overline{\mathbb{CP}}^2$ admit genus–1 simplified trisections, any connected sum of them with two summands admits a genus–2 simplified trisection. Furthermore, we can deduce from [6, Theorem 1.4] that $S^2 \times S^2$ also admits a genus–2 simplified trisection. These observations prove the if part of the theorem, so we will prove the only if part.

Let $f : X \to \mathbb{R}^2$ be a simplified $(2, k)$–trisection ($k = 0, 1, 2$). The manifold X is diffeomorphic to $\sharp^2(S^1 \times S^3)$ if k is equal to 2 (see [9, Remark 5]). Assume that k is not equal to 2. We take vanishing cycles a_1, a_2 and b_j, c_j ($j = 1, \ldots, g - k$) in $\Sigma = \Sigma_2$ as we took in Theorem 3.4. By changing the orientation of X if necessary, we can assume that there are orientations of a_1, b_1 and c_1 such that the algebraic intersections $a_1 \cdot b_1, b_1 \cdot c_1$ and $c_1 \cdot a_1$ are equal to 1. Let $\Sigma' \subset \Sigma$ be a regular neighborhood of $a_1 \cup b_1 \cup c_1$, which is a genus–1 surface with three boundary components by Lemma 3.6. We denote the three boundary components of Σ' by δ_1, δ_2 and δ_3 as shown in Figure 6(1). If $k = 1$, we can deduce from Theorem 3.4 and Lemma 3.6 that the product $t_{\delta_1}^2 t_{\delta_3}^2 t_{\delta_2}^{-1}$ (which is regarded as an element in $\text{Mod}(\Sigma_{a_1})$) preserves the isotopy class of a_2. Since Σ_{a_1} is a torus, it is easy to see that a_2 is disjoint from

the curves $\delta_1, \delta_2, \delta_3$, and thus from a_1, b_1, c_1. We can therefore change f by homotopy so that the innermost triangle in $f(\mathrm{Crit}(f))$ is moved to the outermost region (i.e. the region bounded by the definite fold image). We can then apply unwrinkle to the resulting map, which yields a Lefschetz singularity with a trivial vanishing cycle. Thus, the manifold X is a blow-up of a manifold admitting $(1, 1)$–trisection, which is diffeomorphic to $S^1 \times S^3$.

In what follows, we assume that $k = 0$. Since the genus of Σ is 2, we can obtain Σ by capping $\partial \Sigma'$ by either (1) a genus–1 surface with one boundary component and two disks, or (2) an annulus and a disk. For the case (1), either of the components δ_1 and δ_3 bounds a disk in Σ. In particular we can apply unwrinkle to f so that the inner indefinite fold image of f becomes a Lefschetz critical value with a trivial vanishing cycle. Thus X is a blow-up of a 4–manifold admitting a $(1, 0)$–trisection, which is either $\mathbb{CP}^2$ or $\overline{\mathbb{CP}^2}$.

Assume that the components $\delta_1, \delta_2, \delta_3$ bound an annulus and a disk in Σ. By Lemma 3.6 the monodromy $\psi \in \mathrm{Mod}(\Sigma_{a_1})$ along the loop going between the inner and the outer fold images of f is a (single or fourth power of) Dehn twist along an essential simple closed curve d. We take an identification of $H_1(\Sigma_{a_1}; \mathbb{Z})$ with $\mathbb{Z}^2$ so that d represents the element $\left(\begin{smallmatrix} 1 \\ 0 \end{smallmatrix} \right)$. Let $\left(\begin{smallmatrix} p \\ q \end{smallmatrix} \right), \left(\begin{smallmatrix} r \\ s \end{smallmatrix} \right)$ and $\left(\begin{smallmatrix} t \\ u \end{smallmatrix} \right) \in \mathbb{Z}^2$ be elements represented by a_2, b_2 and c_2, respectively. Since a_2 intersects each of the curves b_2 and c_2 on one point, the following equality holds:

$$(1) \qquad ps - qr = pu - qt = 1 \iff \begin{pmatrix} s & -r \\ u & -t \end{pmatrix} \begin{pmatrix} p \\ q \end{pmatrix} = \begin{pmatrix} 1 \\ 1 \end{pmatrix}.$$

If one of the integers q, s, u is equal to zero, one of the curves a_2, b_2 and c_2 is disjoint from the three curves a_1, b_1 and c_1. Thus we can apply a homotopy to f so that the nested indefinite fold images of f becomes two circles bounding disjoint disks as shown in Figure 11. Since a regular fiber inside each of the two circles is a genus–1 surface, we can further apply
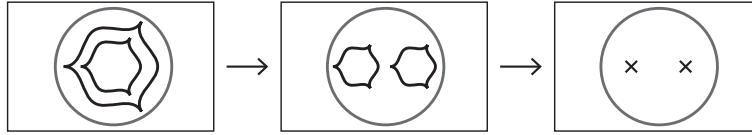

Fig. 11. Homotopies applied to a genus–2 simplified trisection.

wrinkles so that the two indefinite circles become two (possibly achiral) Lefschetz singularities. We can thus conclude that the total space of the original trisection is a connected sum of $\mathbb{CP}^2$ and $\overline{\mathbb{CP}^2}$ with two summands. In what follows we will assume $q, s, u \neq 0$.

If ψ is equal to t_d (i.e. δ_2 is a boundary component of an annulus in $\overline{\Sigma \setminus \Sigma'}$), we can apply unwrinkle to f so that the inner indefinite fold circle becomes a Lefschetz singularity with a vanishing cycle d (see the first two figures in Figure 12). Since the curve $\overline{d}(c_2) = \left(\begin{smallmatrix} t-u \\ u \end{smallmatrix} \right)$ intersects $b_2 = \left(\begin{smallmatrix} r \\ s \end{smallmatrix} \right)$ on one point by Theorem 3.4, we obtain $ur - (t - u)s = \pm 1$ and $ur - ts = -us \pm 1$. Suppose that $ts - ur = -\det \left(\begin{smallmatrix} s & -r \\ u & -t \end{smallmatrix} \right)$ is not equal to 0 and $|q|$ is greater than 1. We can deduce the following inequality from the equality (1):

$$2 \leq |q| = \frac{|s - u|}{|-us \pm 1|}$$
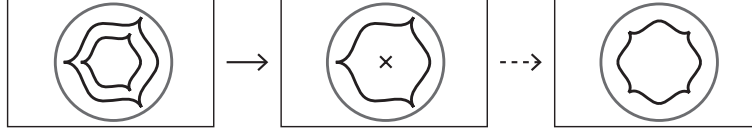$$\Rightarrow 2(|us| - 1) - (|u| + |s|) \leq 0$$

Fig. 12. Homotopies applied to a genus–2 simplified trisection. Note that the second one can be applied only if one of the integers q, s and u is equal to ± 1.

$$\Rightarrow \left(|s| - \frac{1}{2} \right) \left(|u| - \frac{1}{2} \right) \leq \frac{5}{4}.$$

The last inequality implies that either $|s|$ or $|u|$ is equal to 1 (note that we assume $s, u \neq 0$). We can thus conclude that one of the integers q, s, u is equal to ± 1 if $\det \left(\begin{smallmatrix} s & -r \\ u & -t \end{smallmatrix} \right)$ is not equal to 0. If $\det \left(\begin{smallmatrix} s & -r \\ u & -t \end{smallmatrix} \right)$ is equal to 0, we can deduce from the equality (1) that $\left(\begin{smallmatrix} s \\ u \end{smallmatrix} \right)$ is equal to $\pm \left(\begin{smallmatrix} 1 \\ 1 \end{smallmatrix} \right)$.

In any case, one of the curves a_2, b_2 and c_2 intersects d on one point. We can thus apply unsink as shown in Figure 12. Let d_1, d_2, d_3 and d_4 be vanishing cycles of indefinite fold arcs between two of the four cusps. Since two consecutive cycles d_i and d_{i+1} (taking indices mod 4) intersect on one point, it is easy to deduce that either of the followings occurs for some $i \in \mathbb{Z}/4\mathbb{Z}$:

- the cycles d_i and d_{i+2} are disjoint,
- the cycles d_i and d_{i+2} intersect on one point,

In the former case, we can apply flip and slip to f so that the resulting map $\tilde{f}$ does not have cusps. Let $D \subset \mathbb{R}^2$ be a open disk inside the innermost fold image of $\tilde{f}$. It is easy to see that the complement $X \setminus \tilde{f}^{-1}(D)$ admits a trivial bundle over S^1 with a fiber $S^2 \times I$, and X can be obtained from this bundle by attaching two copies of the trivial bundle $S^2 \times D^2$ over D^2 by fiber-preserving diffeomorphisms. We can thus conclude that X is an S^2–bundle over S^2.

Lastly, we will prove that the monodromy ψ never be equal to t_d^4 (i.e. δ_2 never bound a disk in $\overline{\Sigma \setminus \Sigma'}$) under the assumption that $q, s, u \neq 0$. To do this, suppose that ψ would be equal to t_d^4. The curve $_{t_d^4}(c_2) = \left(\begin{smallmatrix} t-4u \\ u \end{smallmatrix} \right)$ would intersect $b_2 = \left(\begin{smallmatrix} r \\ s \end{smallmatrix} \right)$ on one point by Theorem 3.4 and Lemma 3.6. Thus $\det \left(\begin{smallmatrix} s & -r \\ u & -t \end{smallmatrix} \right) = -4us \pm 1$ would not be equal to 0, and we obtain:

$$1 \leq |q| = \frac{|s - u|}{|-4us \pm 1|}$$

$$\Rightarrow (4|us| - 1) - (|u| + |s|) \leq 0$$

$$\Rightarrow \left(2|s| - \frac{1}{2} \right) \left(2|u| - \frac{1}{2} \right) \leq \frac{5}{4}.$$

This contradicts the assumption that s and u are not equal to 0. $\qquad \square$

4. Trisection diagrams from broken Lefschetz fibrations

In [6] the authors gave an explicit algorithm to obtain a simplified trisection from a directed broken Lefschetz fibration. In this section, we first explain how to obtain a trisection *diagram* of a simplified trisection obtained by this algorithm. Although our method works for Lefschetz fibrations and directed broken Lefschetz fibrations, we will only focus on simplified broken Lefschetz fibrations for simplicity. We then apply this method to genus–1

simplified broken Lefschetz fibrations.

We begin with a brief review of the algorithm in [6] mentioned above. Let $f : X \to S^2$ be a genus–g simplified broken Lefschetz fibration with k Lefschetz singularities. We first take a decomposition $S^2 = D_1 \cup D_2 \cup D_3$, where D_1 is a disk including all the critical values of f, $D_3 \subset S^2 \setminus D_1$ is a small disk neighborhood of a regular value with a lower genus fiber and D_2 is an annulus between the two disks. We take identifications $D_2 \cong S^1 \times [-1, 1]$ and $f^{-1}(D_2) \cong S^1 \times [-1, 1] \times \Sigma_{g-1}$ under which the restriction $f|_{f^{-1}(D_2)}$ is the projection onto the former components. Let $h : \Sigma_{g-1} \to [1, 2]$ be a Morse function with $2g - 2$ index–1 critical points, one index–0 critical point and one index–2 critical point. Using h we define $\varphi : [-1, 1] \times \Sigma_{g-1} \to [1, 3]$ as $\varphi(t, x) = 1 + (1 - t^2)h(x)^\dagger$ and $f_1 : X \to \mathbb{R}^2$ as follows: f_1 is a composition of $f|_{f^{-1}(D_i)}$ and a suitable diffeomorphism from D_i to a unit disk $D^2 \subset \mathbb{R}^2$ on $f^{-1}(D_i)$ for $i = 1, 3$, and is a composition of $\mathrm{id}_{S^1} \times \varphi$ and a suitable diffeomorphism from $S^1 \times [1, 3]$ to an annulus in $\mathbb{R}^2$ on $f^{-1}(D_2) \cong S^1 \times [-1, 1] \times \Sigma_{g-1}$. The critical value set of f_1 is as shown in Figure 13(1), where it has $2g - 1$ outward-directed indefinite fold circles. We first apply R2–moves twice to interchange the first and the second innermost circles, yielding the critical value set shown in Figure 13(2). The Lefschetz singularities can be moved to the outside of the innermost region by a homotopy, and the resulting critical value set is shown in Figure 13(3). We can then apply flip and slip and unsink to obtain an indefinite fold circle with three cusps as shown in Figure 13(5). Finally, we can obtain a simplified trisection by applying wrinkles and pushing Lefschetz singularities inside successively. The resulting trisection has $2g-1$ indefinite fold circles without cusps and $k+2$ indefinite fold circles with three cusps, so it is a simplified $(2g + k + 1, 2g - 1)$–trisection.

We denote the map appearing in the algorithm with critical value set Figures 13(2),..., 13(6) by $f_2, \ldots, f_6$, respectively. In order to obtain a trisection *diagram* associated with a simplified trisection constructed above, we have to get vanishing cycles of f_1 and know how these are changed in each of the homotopies applied in the algorithm. Let G' be a Riemannian metric on Σ_{g-1} so that the pair (h, G') satisfies the Morse–Smale condition (for details of this condition, see [2]) and $G = (h(x)dt^2) \oplus G'$, which is a Riemannian metric on $[-1, 1] \times \Sigma_{g-1}$. We first determine stable and unstable manifolds of φ with respect to the metric G.

Lemma 4.1. *Let $\varepsilon > 0$ be a sufficiently small positive number.*

(1) *The fiber $\varphi^{-1}(2+\varepsilon)$ is diffeomorphic to a closed surface obtained by attaching two copies of $h^{-1}([1 + \varepsilon, 2])$ by the identity along the boundary.*

(2) *For the index–0 critical point $x_0 \in \mathrm{Crit}(h)$, the intersection between $\varphi^{-1}(2 + \varepsilon)$ and the stable manifold $W^s(0, x_0)$ of $(0, x_0)$ is the boundary of the two copies of $h^{-1}([1 + \varepsilon, 2])$ under the identification given in the proof of (1).*

(3) *For an index–1 critical point $x \in \mathrm{Crit}(h)$, the intersection between $\varphi^{-1}(2 + \varepsilon)$ and the unstable manifold $W^u(0, x)$ of $(0, x)$ is the union of two copies of the intersection between $h^{-1}([1 + \varepsilon, 2])$ and the unstable manifold $W^u(x)$ of x under the identification given in the proof of (1).*

$\dagger$Here we take a different φ from that in [6] in order to make it easy to take a vector field giving vanishing cycles.
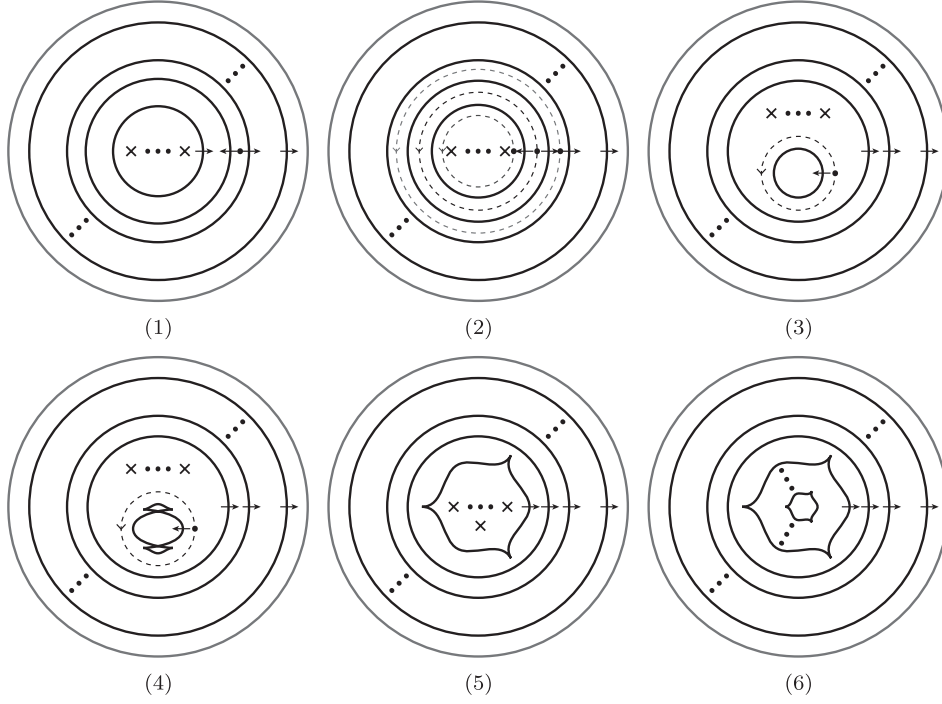
Fig. 13. Critical value sets appearing in the algorithm to obtain a trisection.

Proof. For simplicity, we denote the two copies of the surface $h^{-1}([1 + \varepsilon, 2])$ by Σ'_1 and Σ'_2. It is easy to see that the map $\Phi : \varphi^{-1}(2 + \varepsilon) \to \Sigma'_1 \cup_{\mathrm{id}} \Sigma'_2$ defined as

$$\Phi(t, x) = \begin{cases} x \in \Sigma'_1 & (t \geq 0) \\ x \in \Sigma'_2 & (t \leq 0) \end{cases}$$

is a diffeomorphism, in particular the statement (1) holds. Let $c_p(s)$ be the integral curve of $\mathrm{grad}(h)$ with the initial point $p \in \Sigma_{g-1}$ and $C_{(t,q)}(s) = \left(C^1_{(t,q)}(s), C^2_{(t,q)}(s) \right)$ be the integral curve of $\mathrm{grad}(\varphi)$ with the initial point $(t, q) \in \varphi^{-1}(2 + \varepsilon)$. Since the gradient $\mathrm{grad}(\varphi)$ of φ is equal to $-2t\frac{\partial}{\partial t} + (1 - t^2)\, \mathrm{grad}(h)$, the components $C^1_{(t,q)}(s)$ and $C^2_{(t,q)}(s)$ are respectively equal to $t\exp(-2s)$ and $c_q\left(s - \frac{t^2}{4}(1 - \exp(-4s)) \right)$. Thus, the point $(t, q) \in h^{-1}(1 + \varepsilon)$ is contained in $W^s(0, x_0)$ if and only if $\lim\limits_{s \to -\infty} c_q\left(s - \frac{t^2}{4}(1 - \exp(-4s)) \right) = x_0$ and $\lim\limits_{s \to -\infty} t\exp(-2s) = 0$. We can deduce from the second equality that t is equal to 0. Since $\Phi(0, q)$ is contained in $W^s(x_0)$ (in particular $\lim\limits_{s \to -\infty} c_q(s) = x_0$), the statement (2) holds. Similarly, for an index–1 critical point $x \in \mathrm{Crit}(h)$, the point $(t, q) \in h^{-1}(1 + \varepsilon)$ is contained in $W^u(0, x)$ if and only if $\lim\limits_{s \to \infty} c_q\left(s - \frac{t^2}{4}(1 - \exp(-4s)) \right) = x$ and $\lim\limits_{s \to \infty} t\exp(-2s) = 0$. The second equality holds for any t and the first equality implies that q is contained in $W^u(x)$. This completes the proof of the statement (3). $\square$

By Lemma 4.1 we can obtain vanishing cycles of the map f_1 in a regular fiber on the second innermost annulus (i.e. the fiber on the dot in Figure 13(1)): the blue curve in Fig-

ure 14, which we denote by c, is a vanishing cycle of the second innermost fold circle, red curves are vanishing cycles of the outer fold circles, and the pair of the two shaded disks is a neighborhood of a vanishing set of the innermost fold circle. A regular fiber of f_2 on
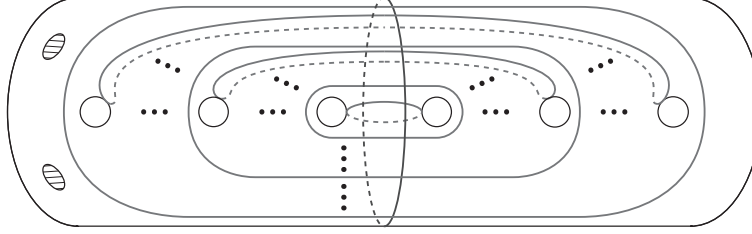

Fig. 14. Vanishing cycles of f_1.

the innermost annulus (i.e. the fiber on the dot in Figure 13(2)) can be obtained by applying surgery along the two shaded disks in Figure 14. We denote this regular fiber by Σ. A vanishing cycle of the second innermost fold circle, which we denote by d, is parallel to the boundary of one of the shaded disks in Figure 14. while the other vanishing cycles are the same as those of f_1.

In order to get vanishing cycles of the maps $f_2, \ldots, f_6$, we need to determine a monodromy $\varphi_2 \in \mathrm{Mod}(\Sigma)$ along a dotted black circle in Figure 13(2). Let $c_1, \ldots, c_k$ be vanishing cycles of the Lefschetz singularities with respect to some Hurwitz path system. We regard these cycles as curves in Σ_c, which is a surface obtained by applying surgery along $c \subset \Sigma$.

Proposition 4.2. *Suppose that g is greater than 2. For any element $\varphi \in \mathrm{Ker}(\Phi_d)$ satisfying the condition $\Phi_c(\varphi) = t_{c_k} \circ \cdots \circ t_{c_1} \in \mathrm{Mod}(\Sigma_c)$, there exist R2–moves applied to f_1 in the algorithm above such that the resulting monodromy φ_2 is equal to φ.*

Proof. We can prove the proposition in a way similar to that of the proof of [12, Theorem 3.9] provided that the following claim holds:

Claim. *The subgroup $\mathrm{Ker}(\Phi_c) \cap \mathrm{Ker}(\Phi_d) \subset \mathrm{Mod}(\Sigma)(c, d)$ is generated by the following set:*

$$\left\{ t_{\tilde{\delta}(\eta)} \circ t_c^{-1} \circ t_d^{-1} \in \mathrm{Mod}(\Sigma)(c, d) \,\middle|\, \begin{array}{l} \eta \in \Pi\left(\Sigma_{c,d} \setminus \{v_i, w_j\}, v_k, w_l\right) \\ \{i, k\} = \{j, l\} = \{1, 2\} \end{array} \right\},$$

where $v_1, v_2 \in \Sigma_{c,d}$ (resp. $w_1, w_2 \in \Sigma_{c,d}$) are the origins of the two disks attached in surgery along c (resp. d), and $\Pi\left(\Sigma_{c,d} \setminus \{v_i, w_j\}, v_k, w_l\right)$ and $\tilde{\delta}(\eta)$ are defined in the same way as in [12, Section 3].

Let F_{v_1, v_2} and F_{w_1, w_2} be the forgetting map defined on $\mathrm{Mod}(\Sigma_{c,d}; v_1, v_2, w_1, w_2)$. To prove the claim, we first observe that the restriction

$$\Phi_c^* \circ \Phi_d^*|_{\mathrm{Ker}(\Phi_c) \cap \mathrm{Ker}(\Phi_d)} : \mathrm{Ker}(\Phi_c) \cap \mathrm{Ker}(\Phi_d) \to \mathrm{Ker}(F_{v_1, v_2}) \cap \mathrm{Ker}(F_{w_1, w_2})$$

is an isomorphism (see the proof of [12, Lemma 3.1]). We denote the connected component of $\Sigma_{c,d}$ containing v_1, w_1, w_2 (resp. v_2) by Σ' (resp. Σ''). It is easy to see that $\mathrm{Ker}(F_{v_1, v_2}) \cap \mathrm{Ker}(F_{w_1, w_2})$ is contained in the kernel of $F_{v_1} : \mathrm{Mod}(\Sigma'; v_1, w_1, w_2) \to \mathrm{Mod}(\Sigma'; w_1, w_2)$, where we regard $\mathrm{Mod}(\Sigma'; v_1, w_1, w_2)$ as a subgroup of the group $\mathrm{Mod}(\Sigma_{c,d}; v_1, v_2, w_1, w_2)$ in the ob-

vious way. Since Σ' is not a sphere, in particular a connected component of $\text{Diff}^+(\Sigma', w_1, w_2)$ is contractible, the kernel of $F_{v_1} : \text{Mod}(\Sigma'; v_1, w_1, w_2) \to \text{Mod}(\Sigma'; w_1, w_2)$ is isomorphic to $\pi_1(\Sigma' \setminus \{w_1, w_2\}, v_1)$. The intersection $\text{Ker}(F_{v_1}) \cap \text{Ker}(F_{w_1, w_2})$ is then isomorphic to the kernel of the map $i_* : \pi_1(\Sigma' \setminus \{w_1, w_2\}, v_1) \to \pi_1(\Sigma', v_1)$ since the diagram

$$
\begin{array}{ccc}
\pi_1(\Sigma' \setminus \{w_1, w_2\}, v_1) & \xrightarrow{\ P_1\ } & \text{Mod}(\Sigma'; v_1, w_1, w_2) \\
i_* \downarrow & & \downarrow F_{w_1, w_2} \\
\pi_1(\Sigma', v_1) & \xrightarrow{\ P_2\ } & \text{Mod}(\Sigma'; v_1)
\end{array}
$$

commutes and the pushing map $P_2 : \pi_1(\Sigma', v_1) \to \text{Mod}(\Sigma'; v_1)$ is injective (note that it would not hold if the genus of Σ' were equal to 1). The rest of the proof of the claim is quite similar to that of [12, Theorem 3.4], so we leave it to the reader. $\qquad\square$

Note that Proposition 4.2 would not hold without the assumption on g. In order to get a monodromy φ_2 of f_2 with small fiber genera, we need to take a section on the annulus bounded by the blue and red dotted circles in Figure 13(2) which intersects with the higher-genus connected component of a regular fiber on the innermost region. Using such a section, we can take a lift $\tilde{\varphi}_2 \in \text{Mod}(\Sigma; x)$ of the monodromy φ_2, and we can prove the following in the same way as that of the proof of Proposition 4.2:

Proposition 4.3. *For any element $\tilde{\varphi} \in \text{Ker}(\Phi_d : \text{Mod}(\Sigma, x)(d) \to \text{Mod}(\Sigma_d, x))$ satisfying the condition $\Phi_c(\tilde{\varphi}) = t_{c_k} \circ \cdots \circ t_{c_1} \in \text{Mod}(\Sigma_c, x)$, there exist R2–moves applied to f_1 in the algorithm above such that the resulting lift $\tilde{\varphi}_2$ is equal to $\tilde{\varphi}$.*

We can regard the vanishing cycles $c_1, \ldots, c_k$ as curves in Σ and these are also vanishing cycles of the Lefschetz singularities of f_3. As shown in [12, Figure 6], a regular fiber on the dot in the upper triangle in Figure 15(1), which we denote by $\tilde{\Sigma}$, can be obtained by applying surgery on a pair of disks in Σ. We denote by $\varphi_4 \in \text{Mod}(\Sigma)$ the monodromy along the dotted
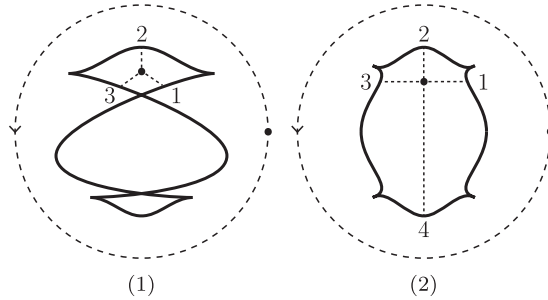

Fig. 15. Parts of critical value sets (1) before and (2) after an R2–move applied to f_4.

circle in Figure 15, which is equal to $\varphi_2 \circ t_{c_1}^{-1} \circ \cdots \circ t_{c_k}^{-1}$. Let $e_i \subset \tilde{\Sigma}$ be a vanishing cycle associated with a reference path in Figure 15(2) labeled by i ($i = 1, 2, 3, 4$). Although we can easily obtain e_1, e_2, e_3 (see [12, Figure 6]), e_4 depends on φ_4:

Proposition 4.4. *Suppose that g is greater than 2. For any element $\psi \in \text{Ker}(\Phi_{e_3}) \cap \text{Mod}(\tilde{\Sigma})(e_1)$ satisfying the condition $\Phi_{e_1}(\psi) = \varphi_4$, there exists an R2–move applied to f_4 such that the resulting vanishing cycle e_4 is equal to $\psi(e_2)$.*

Proposition 4.4 immediately follows from [12, Theorem 4.1].

Again, in order to get e_4 when the genus of a fiber is small, we have to take sections of f_4 on the disk bounded by the dotted circle in Figure 15. The complement $\tilde{\Sigma} \setminus (e_1 \cup e_3)$ has two connected components Σ_h and Σ_l, where the genus of Σ_h is one larger than that of Σ_l. We take a section which intersects with Σ_l if $g = 2$, while we take four sections $\sigma_l^1, \sigma_l^2, \sigma_l^3$ and σ_h so that σ_h (resp. σ_l^i) intersects with Σ_h (resp. Σ_l) if $g = 1$. Using the sections we can take a lift $\tilde{\varphi}_4$ of the monodromy φ_4, which is contained in $\mathrm{Mod}(\tilde{\Sigma}; x)(e_1, e_3)$ if $g = 2$, or in $\mathrm{Mod}(\tilde{\Sigma}; x_1, x_2, x_3, x_4)(e_1, e_3)$ if $g = 1$.

Proposition 4.5. *For any element $\tilde{\psi}$, which is an element in $\mathrm{Ker}(\Phi_{e_3}) \cap \mathrm{Mod}(\tilde{\Sigma}; x)(e_1)$ if $g = 2$ or in $\mathrm{Ker}(\Phi_{e_3}) \cap \mathrm{Mod}(\tilde{\Sigma}; x_1, x_2, x_3, x_4)(e_1)$ if $g = 1$, satisfying the condition $\Phi_{e_1}(\tilde{\psi}) = \tilde{\varphi}_4$, there exists an R2–move applied to f_4 such that the resulting vanishing cycle e_4 is equal to $\tilde{\psi}(e_2)$.*

We can prove Proposition 4.5 as the author proved the theorems in [12, Section 5].

We can regard the vanishing cycles $c_1, \ldots, c_k$ as curves in $\tilde{\Sigma}$, and these are also vanishing cycles of Lefschetz singularities of f_5. It is also easy to obtain a vanishing cycle of a Lefschetz singularity appearing when applying unsink to obtain f_5. The simplified trisection f_6 can be obtained by applying wrinkles and pushing Lefschetz singularities across indefinite folds. Since we can easily understand how vanishing cycles are changed by these moves (for wrinkles, see [7, Figure 8]), we can eventually obtain a trisection diagram associated with the trisection f_6.

EXAMPLE 4.6. Here we will apply the algorithm above to genus–1 simplified broken Lefschetz fibrations without Lefschetz singularities. Such fibrations were first given in [1] and then completely classified in [5, 11]: a 4–manifold X admits a genus–1 simplified broken Lefschetz fibration without Lefschetz singularities if and only if X is diffeomorphic to one of the manifolds $S^4, S^1 \times S^3 \sharp S^2 \times S^2, S^1 \times S^3 \sharp \mathbb{CP}^2 \sharp \overline{\mathbb{CP}^2}, L_n$ and L'_n, where L_n and L'_n ($n \geq 2$) are 4–manifolds introduced in [15][‡]. For simplicity of the notations, we put $L_1 = L'_1 = S^4$, $L_0 = S^1 \times S^3 \sharp S^2 \times S^2$ and $L'_0 = S^1 \times S^3 \sharp \mathbb{CP}^2 \sharp \overline{\mathbb{CP}^2}$.

Let $f : X \to S^2$ be a genus–1 simplified broken Lefschetz fibration without Lefschetz singularities and $f_1 : X \to \mathbb{R}^2$ be a map appearing when applying the algorithm to f (the critical value set of f_1 is shown in Figure 16(1)). Let $\nu(f(\mathrm{Crit}(f)))$ be a tubular neighborhood of $f(\mathrm{Crit}(f)) \subset S^2$. Since the composition of the restriction $f|_{\nu(f(\mathrm{Crit}(f)))}$ and the natural projection $\nu(f(\mathrm{Crit}(f))) \to f(\mathrm{Crit}(f))$ is a trivial bundle, the composition of the restriction
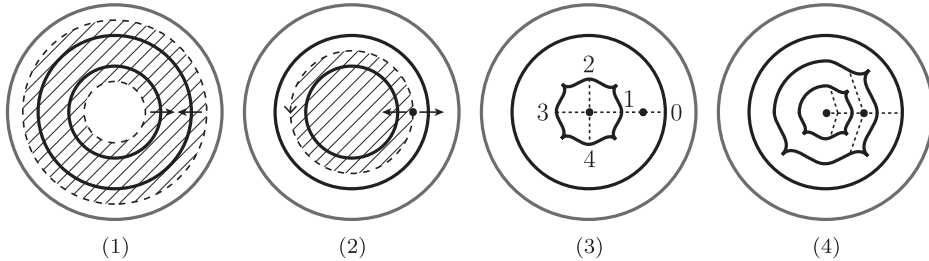

Fig. 16. Critical value sets of (1) f_1, (2) f_2, (3) f_4 and (4) f_6.

[‡]In this paper, we assume that a simplified broken Lefschetz fibration has indefinite folds.

of f_1 on the preimage of the shaded annulus in Figure 16(1) and a retraction to one of the boundary components of the annulus is also a trivial bundle. Thus we can take a section σ of f_1 over the shaded annulus in Figure 16(1) so that the resulting lifted monodromies (which are contained in the mapping class groups of pointed surfaces) along the two boundary components are both trivial. By proposition 4.3 we can apply R2–moves to f_1 so that the monodromy along the boundary of the shaded disk in Figure 16(2) is trivial.

There exists a genus–1 simplified broken Lefschetz fibration $f_0 : L_0 \to S^2$ such that a section σ above can be taken so that it can be extended to the inside of the shaded annulus in Figure 16(1). We take four sections $\sigma_1, \ldots, \sigma_4$ of $f_{0,2}$ over the shaded disk in Figure 16(2) so that one of them intersects the torus component of the central fiber, while the others intersect the sphere component of it. We also take two regular values of $f_{0,4}$ as shown in Figure 16(3). We can obtain vanishing cycles $e_0, \ldots, e_4$ associated with the reference paths in Figure 16(3), together with points corresponding to sections as shown in Figures 17(1) and 17(2).
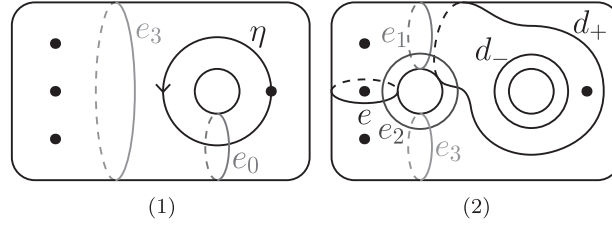

(1)   (2)

Fig. 17. Regular fibers of $f_{0,2}$. Note that e_4 is equal to e_2 for $f_{0,2}$.

A map $f_{n,2} : L_n \to \mathbb{R}^2$ derived from a genus–1 simplified broken Lefschetz fibration $f_n : L_n \to S^2$ can be obtained from $f_{0,2}$ by applying multiplicity–1 logarithmic transformation along the torus component of the central fiber with the direction η (which is described in Figure 17(1)) and the auxiliary multiplicity n (for the definition of the direction and the auxiliary multiplicity of a logarithmic transformation, see [10, Section 8.3]). Furthermore, we can obtain $f'_{n,2}$ derived from a genus–1 fibration $f'_n : L'_n \to S^2$ from f_n by applying Gluck twist along the sphere component of the central fiber. We can thus deduce from Proposition 4.5 that the vanishing cycle of $f_{n,4}$ associated with the reference path labeled by 4 (see Figure 16(3)) is $\psi_n(e_2)$, while that of $f'_{n,4}$ is $\psi'_n(e_2)$, where $\psi_n = t^n_{d_+} t^{-n}_{d_-}$, $\psi'_n = t^n_{d_+} t^{-n}_{d_-} t_e$ and d_+, d_-, e, e_2 are curves given in Figure 17(2).

Applying unsink to the cusp between the reference paths labeled by 2 and 3, and wrinkle to the resulting Lefschetz singularity, we can finally obtain a $(3, 1)$–trisection whose critical value set is shown in Figure 16(4). Figure 18(1) describes vanishing cycles of $f_{0,6}$ in a fiber of the point outside of the innermost triangle in Figure 16(4), where the central fiber can be obtained by applying surgery on the two red disks (we can obtain this diagram by embedding a diagram in [7, Figure 8] in a suitable way). Using the diagram in Figure 18(1), we can further obtain vanishing cycles $a_1, a_2, a_3, b_1, b_2, c_1, c_2$ of $f_{0,6}$ obtained by following the procedure in the beginning of Section 3: a_i, b_i and c_i are the red, blue and green curves in Figures 18(2) and 18(3) with label i, respectively. It is easy to see that the surgeries changing f_0 to f'_n (that is, logarithmic transformations and Gluck twists) do not affect the curves a_i's, b_i's and c_1 (i.e. curves in Figure 18(2)). These surgeries change only $c_{0,2} = c_2$ to $c_{n,2} =$
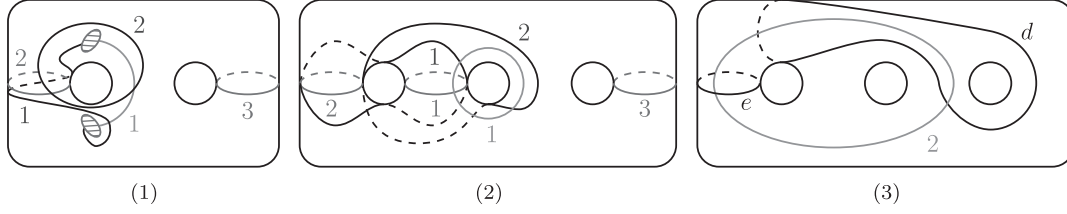
Fig. 18. Vanishing cycles of $f_{0,4}$.

$t_d^n(c_{0,2})$ or $c'_{n,2} = t_d^n t_e(c_{0,2})$. Applying Proposition 3.1, we can eventually obtain trisection diagrams $(\Sigma_3; \alpha_n, \beta_n, \gamma_n)$ and $(\Sigma_3; \alpha'_n, \beta'_n, \gamma'_n)$ associated with $f_{n,6}$ and $f'_{n,6}$, respectively, where

- $(\alpha_n)_i = (\alpha'_n)_i = a_i$ and $(\beta_n)_j = (\beta'_n)_j = b_j$ for each $i = 1, 2, 3$ and $j = 1, 2$ (note that b_2 is disjoint from b_1),
- $(\beta_n)_3 = (\beta'_n)_3 = a_3$, $(\gamma_n)_1 = c_1$, $(\gamma_n)_2 = c_{n,2}$ and $(\gamma'_n)_2 = c'_{n,2}$,
- $(\gamma_n)_3$ (resp. $(\gamma'_n)_3$) can be obtained from a_3 by applying handle-slides (over a_1 and a_2) so that the resulting curve is disjoint from $(\gamma_n)_1$ and $(\gamma_n)_2$ (resp. $(\gamma'_n)_1$ and $(\gamma'_n)_2$).

Some examples of such diagrams are shown in Figure 19. We can put $(\gamma_0)_3 = (\gamma'_0)_3 = a_3$ since $c_{0,2}$ and $c'_{0,2}$ are disjoint from a_3, while we should slide a_3 over a_2 once to obtain $(\gamma_1)_3$ since a_3 intersects $(\gamma_1)_2 = c_{1,2}$.
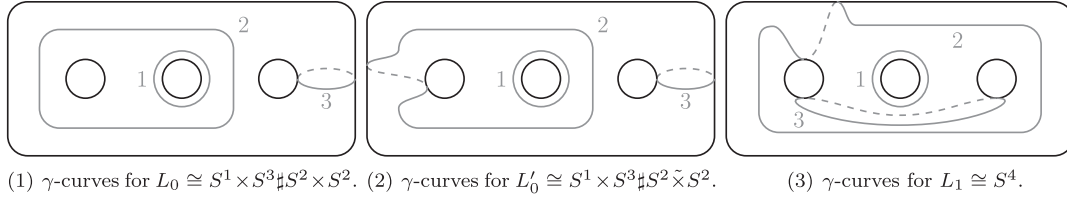
(1) γ-curves for $L_0 \cong S^1 \times S^3 \sharp S^2 \times S^2$. (2) γ-curves for $L'_0 \cong S^1 \times S^3 \sharp S^2 \tilde{\times} S^2$. (3) γ-curves for $L_1 \cong S^4$.

Fig. 19. γ-curves of trisection diagrams associated with simplified trisections.

Using the diagram we can prove that the $(3, 1)$–trisection of S^4 obtained from a genus–1 simplified broken Lefschetz fibration is diffeomorphic to the standard $(3, 1)$–trisection of S^4 (i.e. the stabilization of the $(0, 0)$–trisection, whose diagram is given in [9, Figure 2]) as follows. First, by applying a diffeomorphism of Σ_3 representing $t_{(\gamma_1)_1} t_{(\alpha_1)_1} t_{(\gamma_1)_1}$ to the trisection diagram of S^4 obtained above, we can obtain another (but equivalent) diagram, which is shown in Figure 20(1). We then apply handle-slides as indicated by the dotted arrows in Figure 20(1). The resulting diagram is shown in Figure 20(2). We further apply handle-slides to β–curves as indicated by the dotted arrows in Figure 20(2). We eventually obtain the diagram in Figure 20(3), which is obviously equivalent to the standard $(3, 1)$–
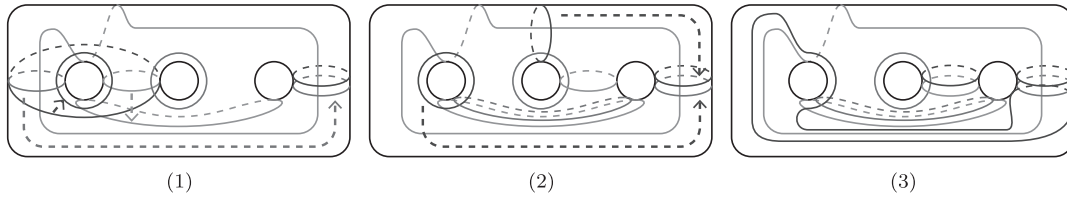
Fig. 20. $(3, 1)$–trisection diagrams of S^4.

trisection diagram of S^4. Similarly, we can also prove that the $(3, 1)$–trisections of L_0 and L_0' obtained from genus–1 simplified broken Lefschetz fibrations are diffeomorphic to a connected sum of the $(1, 1)$–trisection of $S^1 \times S^3$ and the $(2, 0)$–trisections of S^2–bundles over S^2.

References

[1] D. Auroux, S.K. Donaldson and L. Katzarkov: *Singular Lefschetz pencils*, Geom. Topol. **9** (2005), 1043–1114.

[2] A. Banyaga and D. Hurtubise: Lectures on Morse homology, Kluwer Texts in the Mathematical Sciences, **29**, Kluwer Academic Publishers Group, Dordrecht, 2004.

[3] R. İ. Baykur: *Topology of broken Lefschetz fibrations and near-symplectic four-manifolds*, Pacific J. Math. **240** (2009), 201–230.

[4] R.İ. Baykur and K. Hayano: *Broken Lefschetz fibrations and mapping class groups*, Geom. Topol. Monogr. **19** (2015), 269–290.

[5] R.İ. Baykur and S. Kamada: *Classification of broken Lefschetz fibrations with small fiber genera*, J. Math. Soc. Japan, **67** (2015), 877–901.

[6] R.İ. Baykur and O. Saeki: *Simplifying indefinite fibrations on* 4*-manifolds*, preprint, available at arXiv:1705.11169.

[7] S. Behrens and K. Hayano: *Elimination of cusps in dimension 4 and its applications*, Proc. Lond. Math. Soc. (3) **113** (2016), 674–724.

[8] C.J. Earle and A. Schatz: *Teichmüller theory for surfaces with boundary*, J. Differential Geom. **4** (1970), 169–185.

[9] D. Gay and R. Kirby: *Trisecting* 4*-manifolds*, Geom. Topol. **20** (2016), 3097–3132.

[10] R.E. Gompf and A.I. Stipsicz: 4-Manifolds and Kirby Calculus, Graduate Studies in Mathematics **20**, American Mathematical Society, 1999.

[11] K. Hayano: *On genus-1 simplified broken Lefschetz fibrations*, Algebr. Geom. Topol. **11** (2011), 1267–1322.

[12] K. Hayano: *Modification rule of monodromies in an R_2-move*, Algebr. Geom. Topol. **14** (2014), 2181–2222.

[13] J. Meier: *Trisections and spun* 4*-manifolds*, preprint, available at arXiv:1708.01214.

[14] J. Meier and A. Zupan: *Genus-two trisections are standard*, Geom. Topol. **21** (2017), 1583–1630.

[15] P.S. Pao: *The topological structure of 4-manifolds with effective torus actions. I*, Trans. Amer. Math. Soc. **227** (1977), 279–317.

Department of Mathematics
Faculty of Science and Technology
Keio University
Yagami Campus: 3–14–1 Hiyoshi
Kohoku-ku, Yokohama, 223–8522
Japan
e-mail: k-hayano@math.keio.ac.jp